AD-A063 920 ILLINOIS UNIV AT URBANA-CHAMPAIGN ELECTROMAGNETICS LAB F/G 9/5
MULTIMODED WAVEGUIDE COMPONENTS FOR MILLIMETER WAVE INTEGRATED --ETC(U)
SEP 78 S BHOOSHAN DAAG29-77-G-0111
UNCLASSIFIED UIEM-78-10 ARO-14686.2-EL NL

| OF |
AD
A063920

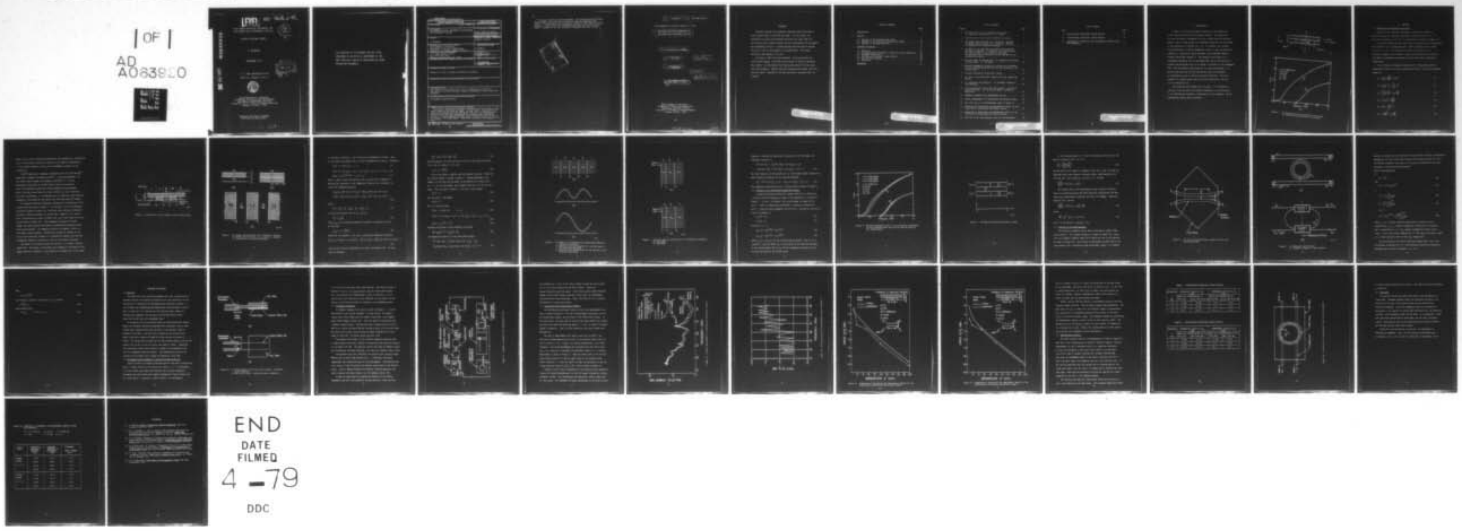

END
DATE
FILMED
4 -79
DDC

ARO 14686.2-EL

(12)

SC

MULTIMODED WAVEGUIDE COMPONENTS FOR MILLIMETER WAVE INTEGRATED CIRCUITS

INTERIM TECHINAL REPORT

S. BHOOSHAN

SEPTEMBER 1978

U. S. ARMY RESEARCH OFFICE

GRANT NO. DAAG29-77-G0111

ELECTROMAGNETICS LABORATORY
DEPARTMENT OF ELECTRICAL ENGINEERING
ENGINEERING EXPERIMENT STATION
UNIVERSITY OF ILLINOIS AT URBANA-CHAMPAIGN
URBANA, ILLINOIS 61801

THE FINDINGS IN THIS REPORT ARE NOT TO BE CONSTRUED AS AN OFFICIAL DEPARTMENT OF THE ARMY POSITION, UNLESS SO DESIGNATED BY OTHER AUTHORIZED DOCUMENTS.

UNCLASSIFIED

SECURITY CLASSIFICATION OF THIS PAGE (When Data Entered)

REPORT DOCUMENTATION PAGE		READ INSTRUCTIONS BEFORE COMPLETING FORM
1. REPORT NUMBER	2. GOVT ACCESSION NO.	3. RECIPIENT'S CATALOG NUMBER
4. TITLE (and Subtitle) MULTIMODED WAVEGUIDE COMPONENTS FOR MILLIMETER WAVE INTEGRATED CIRCUITS		5. TYPE OF REPORT & PERIOD COVERED Interim Technical Report 6. PERFORMING ORG. REPORT NUMBER EM78-10;UILU-ENG-78-2552
7. AUTHOR(s) S. Bhooshan		CONTRACT OR GRANT NUMBERS(s) DAAG29-77-G-0111
9. PERFORMING ORGANIZATION NAME AND ADDRESS Electromagnetics Laboratory Department of Electrical Engineering University of Illinois, Urbana, Illinois		10. PROGRAM ELEMENT, PROJECT, TASK AREA & WORK UNIT NUMBERS P-14686-EL
11. CONTROLLING OFFICE NAME AND ADDRESS U. S. Army Research Office Post Office Box 12211 Research Triangle Park, NC 27709		12. REPORT DATE September, 1978 13. NUMBER OF PAGES 40
14. MONITORING AGENCY NAME & ADDRESS(if different from Controlling Office)		15. SECURITY CLASS. (of this report) UNCLASSIFIED 15a. DECLASSIFICATION/DOWNGRADING SCHEDULE NA

16. DISTRIBUTION STATEMENT (of this Report)

Approved for public release; distribution unlimited.

17. DISTRIBUTION STATEMENT (of the abstract entered in Block 20, if different from Report)

18. SUPPLEMENTARY NOTES

The findings in this report are not to be construed as an official Department of the Army position, unless so designated by other authorized documents.

19. KEY WORDS (Continue on reverse side if necessary and identify by block number)

multimodes; passive devices

20. ABSTRACT (Continue on reverse side if necessary and identify by block number)

Dielectric guides with convenient dimensions have been known to carry several modes in the 60-90 GHz range. In this report, the possibility of using the multimoded inverted strip guide (ISG) for the construction of passive devices has been investigated for millimeter-wave integrated circuits. A simple approach has been used to analyze the ISG, in that it was assumed to be single moded. With proper excitation this appears to be true.
(cont.)

DD FORM 1 JAN 73 1473 EDITION OF 1 NOV 65 IS OBSOLETE

UNCLASSIFIED

SECURITY CLASSIFICATION OF THIS PAGE (When Data Entered)

Two types of ISG's have been examined: the quartz-teflon and teflon-teflon guides. With each type of guide two passive components were tested: the distributed line directional coupler and the single pole ring resonator. Results have been presented which agree quite well with the theory. Analysis of the ISG and passive components has been included.

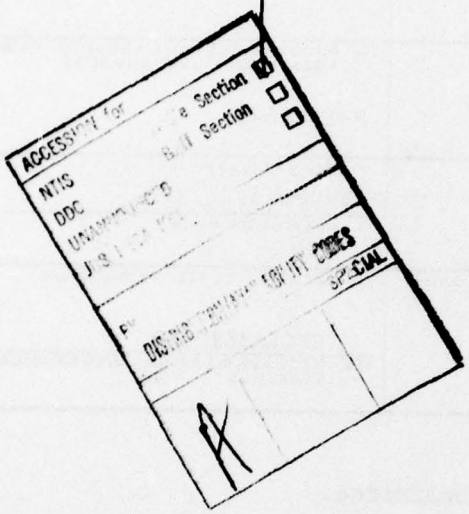

(14) UIEM-78-10, UILU-ENG-78-2552

Electromagnetics Laboratory Report No. 78-10

(6) MULTIMODED WAVEGUIDE COMPONENTS FOR MILLIMETER WAVE INTEGRATED CIRCUITS.

(9) Interim Technical Report,

(10) S. Bhooshan

(12) 42 p.

(11) September 1978

(18) ARO

(19) 14686.2-EL

U.S. Army Research Office
Grant No. (15) DAAG29-77-G-0111

Electromagnetics Laboratory
Department of Electrical Engineering
Engineering Experiment Station
University of Illinois at Urbana-Champaign
Urbana, Illinois 61801

408 102

ABSTRACT

Dielectric guides with convenient dimensions have been known to carry several modes in the 60-90 GHz range. In this report, the possibility of using the multimoded inverted strip guide (ISG) for the construction of passive devices has been investigated for millimeter-wave integrated circuits. A simple approach has been used to analyze the ISG, in that it was assumed to be single-moded. With proper excitation this appears to be true.

Two types of ISG's have been examined: the quartz-teflon and teflon-teflon guides. With each type of guide two passive components were tested: the distributed line directional coupler and the single pole ring resonator. Results have been presented which agree quite well with the theory. Analysis of the ISG and passive components has been included.

TABLE OF CONTENTS

LIST OF FIGURES

LIST OF TABLES

1. INTRODUCTION

A family of dielectric guiding structures for millimeter-wave circuit applications has been previously studied. The integration of active and passive components into such a guide would be desirable. However, most of these guides with reasonable dimensions are multimoded, at the frequencies of interest [1], [2]. For example, the inverted strip guide (ISG), of typical dimensions 4 mm by 1.5 mm, and dielectric constant 2.1, supports at least two modes in the frequency range of interest (60-90 GHz) (Figure 1). The purpose of this paper is to investigate components for the multimoded ISG, and to show that for a properly excited guide, most of the energy is confined to the fundamental mode. The ISG appears single moded for all practical purposes. It may be noted here that the ISG has been set apart as the object of investigation since it has many attractive features: low loss, presence of a ground plane, ease of accurate fabrication, very low cost of fabrication [3].

This paper has been divided into two parts: 1) a theoretical analysis of the ISG and of the passive components to be constructed, 2) the experimental procedure, a description of the apparatus, and the experimental results with conclusions.

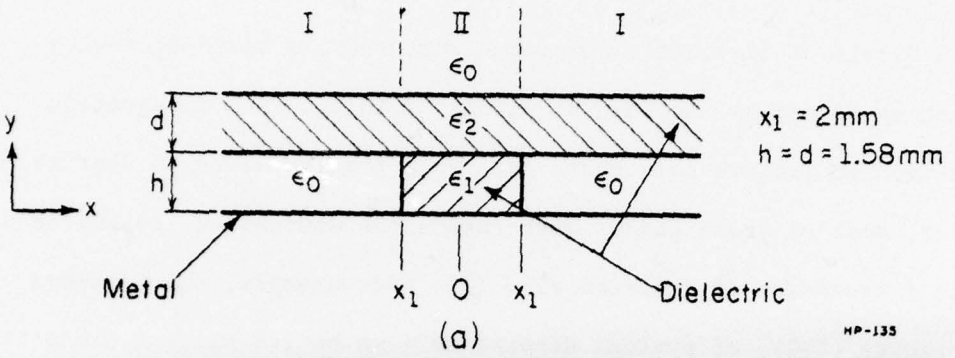

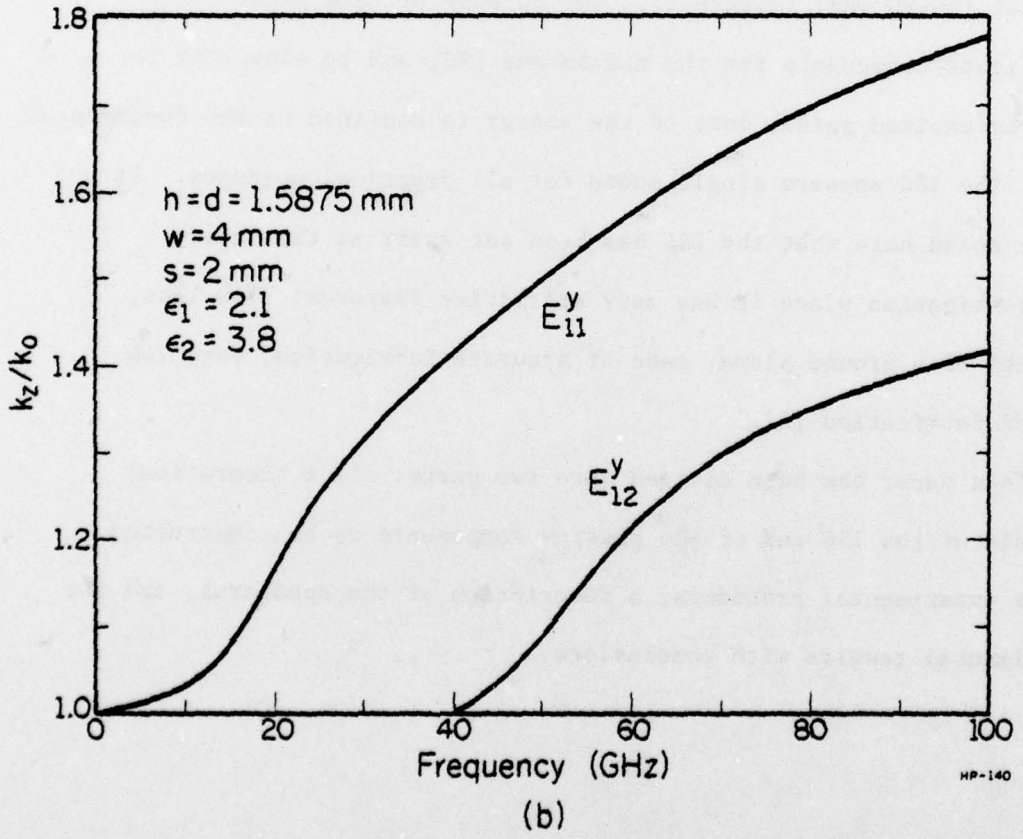

Figure 1. (a) Cross section of the inverted strip guide.
(b) Dispersion characteristic of the guide.

2. ANALYSIS

2.1 Analysis of the Inverted Strip Guide

Analysis of the inverted strip guide is based on the method of effective dielectric constants, developed by Knox and Toulios [4]. It was first described by Itoh [5]; its cross-section is shown in Figure 1(a).

It has been established that there are two possible field configurations, $E_x^{p,q}$ and $E_y^{p,q}$, for a propagating mode. These configurations are hybrid in nature [1], [5]. The subscripts indicate the direction of the principal component of the electric field, and the superscripts indicate the number of extrema of the electric field in the x and y directions, respectively.

If the solution of Maxwell's equations for a rectangular guide is expressed in terms of two scalar potentials ψ^e and ψ^h, the field components become [6]

$$E_x = \frac{1}{\varepsilon_r(y)} \frac{\partial^2 \psi^e}{\partial y \partial x} + \omega \mu k_z \psi^h \tag{1}$$

$$E_y = \frac{1}{\varepsilon_r(y)} \left(k_z^2 - \frac{\partial^2}{\partial x^2}\right) \psi^e \tag{2}$$

$$E_z = \frac{-jk_z}{\varepsilon_r(y)} \frac{\partial \psi^e}{\partial y} - j\omega\mu \frac{\partial \psi^h}{\partial x} \tag{3}$$

$$H_x = -\omega \varepsilon k_z \psi^e + \frac{\partial^2 \psi^h}{\partial y \partial x} \tag{4}$$

$$H_y = \left(k_z^2 - \frac{\partial^2}{\partial x^2}\right) \psi^h \tag{5}$$

$$H_z = j\omega\varepsilon \frac{\partial \psi^e}{\partial x} - jk_z \frac{\partial \psi^h}{\partial y} \tag{6}$$

where ε and μ are the free-space permittivity and permeability, respectively. $\varepsilon_r(y)$ is the relative dielectric constant in the region of application, ω is the radian frequency, and k_z is the propagation constant in the z direction.

The $E_y^{p,q}$ modes have a dominant contribution from ψ^e, while the $E_x^{p,q}$ modes have a dominant contribution from ψ^h. A good approximation for the former types of modes can be made by setting $\psi^h = 0$. We are particularly interested in the $E_y^{p,q}$ modes, since we are going to excite the dielectric guide from a metal waveguide, whose dominant mode is the TE_{01} mode, where the electric field is in the y direction, with just one extremum. It is expected that the transition from the metal waveguide to the dielectric may excite only the lower-order $E_y^{p,q}$ modes.

To analyze the inverted stripguide, consider the cross-section of the coupled structure shown in Figure 2. We can model it as a five-layered structure as shown in Figure 3(c), with each layer having an "effective" dielectric constant obtained in a special way. Regions I, III, and IV have a cross-section as shown in Figure 3(a), and II and V have the cross-section shown in Figure 3(b). The propagation constants for these single- and double-layered structures are determined by matching fields across each boundary: the tangential electric and magnetic fields, on both sides of each boundary. The effective dielectric constant is the value of the dielectric constant of a hypothetical medium, such that the propagation constant is identical to that of the original structure.

The steps of the analysis have been outlined. To proceed, consider Figure 3(b). Since most of the energy will propagate in the region of the higher dielectric constant, it can therefore be assumed that in the region

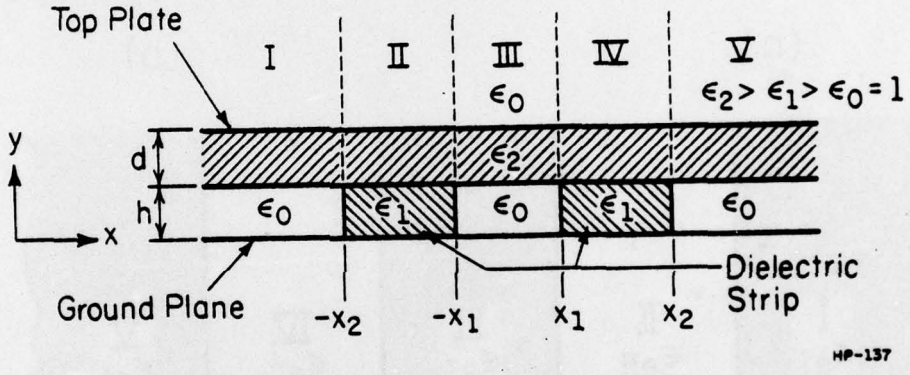

Figure 2. Cross section of the coupled inverted strip guide.

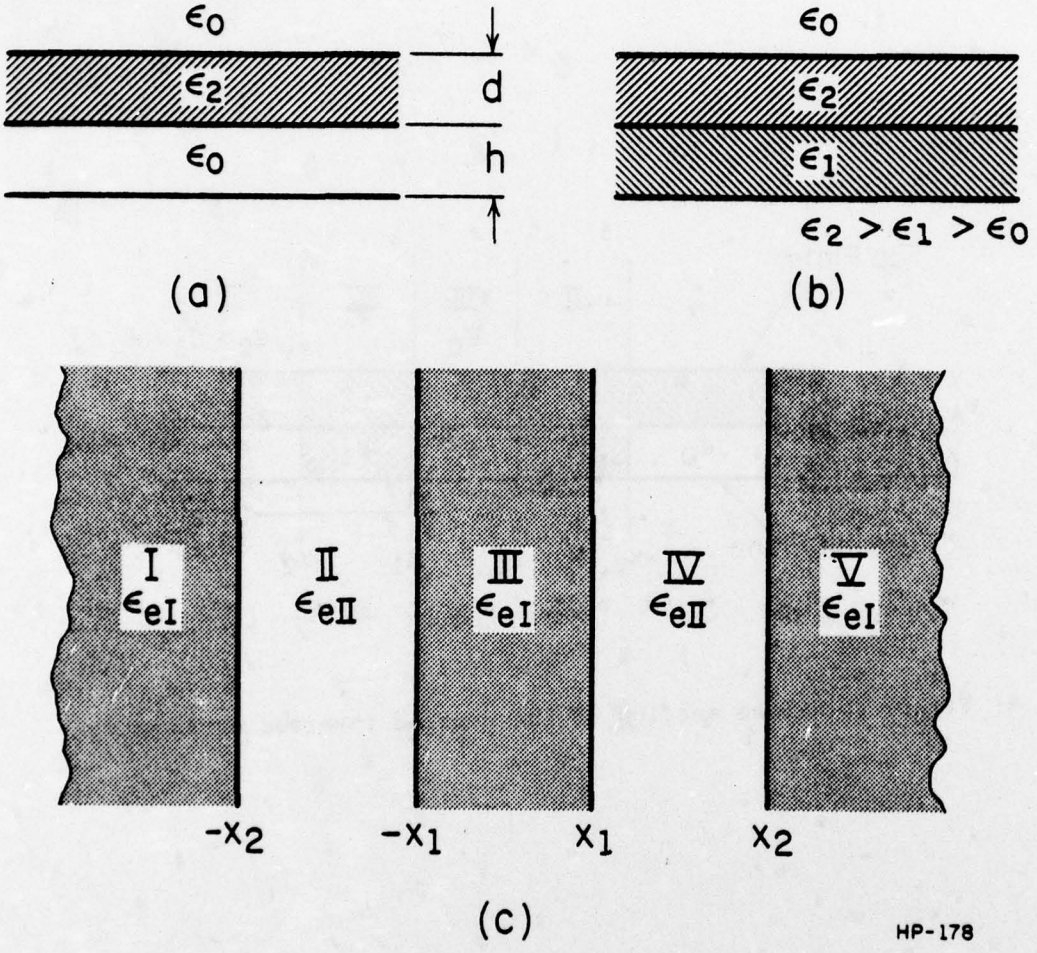

Figure 3. (a) Single slab structure, for y variation analysis.
(b) Double slab structure, for y variation analysis.
(c) Structure for x variation analysis.

of dielectric constant ε_2, the field will be sinusoidal in nature. Also, in the lowest and highest slab, it will be exponential in nature. Therefore,

$$\psi^e(y) = A \cosh(\eta_1 y) \quad , y < h \tag{7}$$

$$\psi^e(y) = B \cos[k_y(y - h)] + c \sin[k_y(y - h)] \quad , h < y < h + d \tag{8}$$

$$\psi^e(y) = D\, e^{-\eta_3(y-h-d)} \quad , y > h + d \quad . \tag{9}$$

Here, η_3 must be real and positive, and η_1 can be real or imaginary. Applying the continuity of the tangential fields at each interface, we obtain the eigenvalue equation:

$$k_y\varepsilon_1\varepsilon_2\eta_3 \cosh(\eta_1 h) \cos(k_y d) + \varepsilon_2^2\eta_1\eta_3 \sinh(y_1 h) \sin(k_y d)$$
$$+ k_y^2\, \varepsilon_1 \cosh(y_1 h) \sin(k_y d) + k_y\varepsilon_2\eta_1 \sinh(\eta_1 h) \cos(k_y d) = 0 \quad . \tag{10}$$

Using

$$k_z^2 = \varepsilon_o k_o^2 + \eta_3^2 = \varepsilon_2 k_0^2 - k_y^2 = \varepsilon_1 k_0^2 + \eta_1^2 \quad , \tag{11}$$

we can solve Equation (10) for k_y, and let

$$k_z^2 = \varepsilon_{eII} k_0^2 \tag{12}$$

where ε_{eII} is the effective dielectric constant of regions II and IV. We find that

$$\varepsilon_{eII} = \varepsilon_2 - k_y^2/k_0^2 \quad . \tag{13}$$

Similarly, for regions I, III, and V, we have the eigenvalue equation:

$$\bar{k}_y\varepsilon_2\bar{\eta}_1 \cos(\bar{k}_y d)\{1 + \tan h(\bar{\eta}_1 h)\} - \bar{k}_y^2 \cos(\bar{k}_y d) + \varepsilon_2^2\bar{\eta}_1^2 \tanh(\bar{\eta}_1 h) \sin(\bar{k}_y d) = 0 \tag{14}$$

where $\bar{k}$ and $\bar{\eta}$ are the counterparts of k and η in Equation (10). We also have the relation:

$$\bar{k}_z^2 = \varepsilon_o k_o^2 + \bar{\eta}_1^2 = \varepsilon_2 k_0^2 - \bar{k}_y^2 \quad . \tag{15}$$

Solving Equation (14) with the help of (15), we can obtain the value of $\bar{k}_y$, and for regions I, III, and V

$$\varepsilon_{eI} = \varepsilon_2 - \bar{k}_y^2/k_0^2 \quad . \tag{16}$$

We are now ready to analyze the five-layered structure. There are two types of modes, as shown in Figure 4. Taking advantage of the symmetry of the even and odd modes, we hypothesize an electric wall at $x = 0$ for the even modes, and a magnetic wall at $x = 0$ for the odd modes. This is shown in Figure 5. For Case I (even modes),

$$E_y(0) = 0 \tag{17}$$

and for Case II (odd modes),

$$H_z(0) = 0 \quad . \tag{18}$$

Now, for the even modes,

$$\psi^e(x) = A \sinh(\xi x) \quad , \quad x < x_1 \tag{19}$$

$$\psi^e(x) = B \cos[k_x(x - x_1)] + C \sin[k_x(x - x_1)] \quad , \quad x_1 < x < x_2 \tag{20}$$

$$\psi^e(x) = D\, e^{-\xi(x - x_2)} \quad . \tag{21}$$

Matching the fields at each interface, and using

$$k_z^2 = \varepsilon_{eI} k_o^2 + \xi^2 = \varepsilon_{eII} k_o^2 - k_x^2 \tag{22}$$

the eigenvalue equation for the even modes becomes

$$[\xi^2 \cosh(\xi x_1) - k_x^2 \sinh(\xi x_1)] \sin[k_x(x_2 - x_1)]$$

$$+ k_x \xi [\cosh(\xi x_1) + \sinh(\xi x_1)] \cos[k_x(x_2 - x_1)] = 0. \tag{23}$$

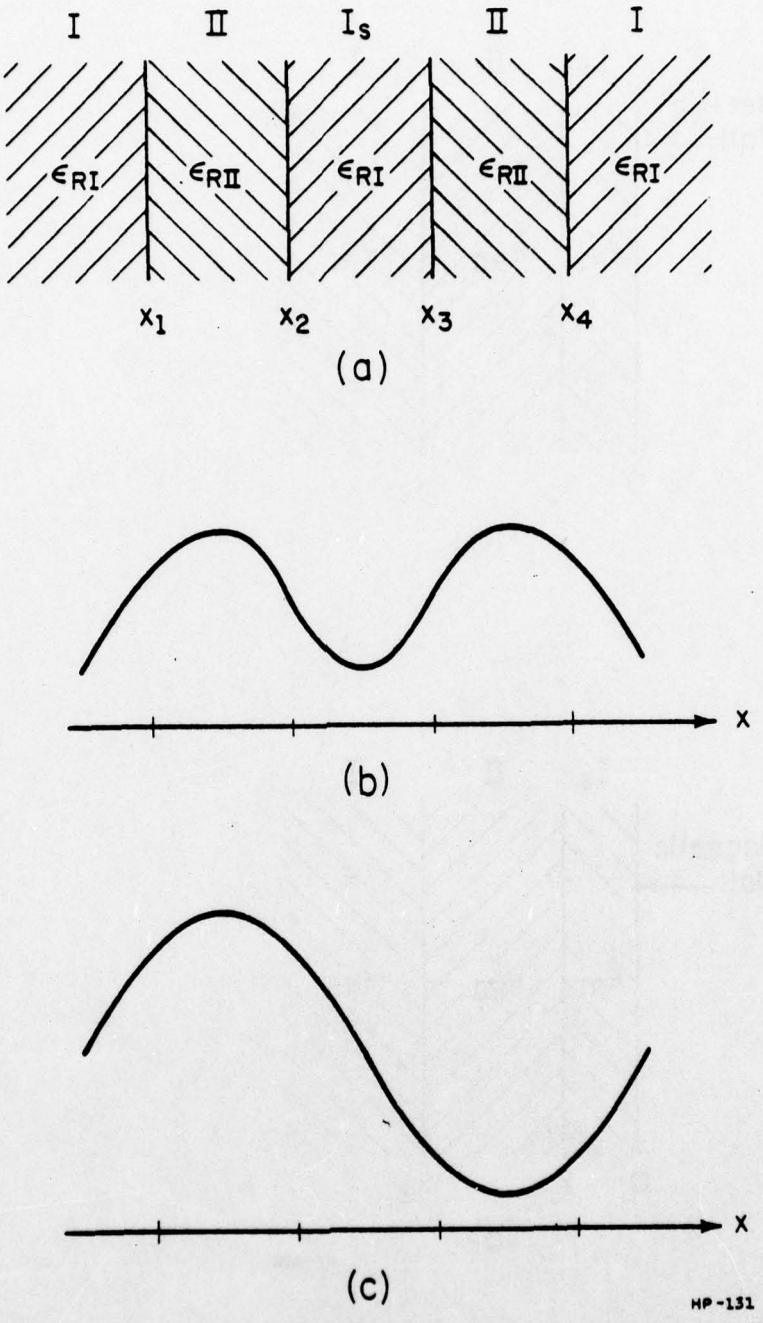

Figure 4. (a) Model of the inverted strip guide using effective dielectric constants.
(b) Relative field distribution for the even mode of the inverted strip guide.
(c) Relative field distribution for the odd mode of the inverted strip guide.

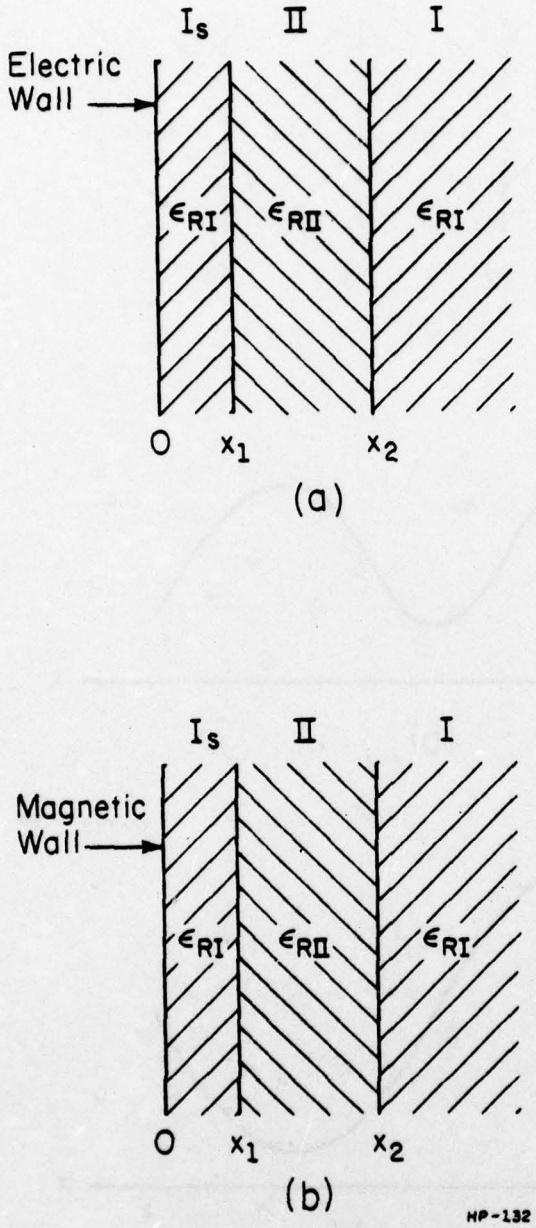

Figure 5. Structure used for derivation of the eigenvalue equations:
(a) Even modes.
(b) Odd modes.

Similarly, carrying the same kind of analysis for the odd modes, the eigenvalue equation is

$$[\xi^2 \sinh(\xi x_1) - k_x^2 \cosh(\xi x_1)] \sin[k_x(x_2 - x_1)]$$

$$+ k_x \xi [\sinh(\xi x_1) + \cosh(\xi x_1)] \cos[k_x(x_2 - x_1)] = 0 \quad . \qquad (24)$$

The above analysis can be applied also to the uncoupled guide, Figure 1(a), whose eigenvalue equation can be obtained similarly:

$$(k_x^2 - \xi^2) \sin[k_x(x_2 - x_1)] - 2\xi k_x \cos[k_x(x_2 - x_1)] = 0 \quad . \qquad (25)$$

The dispersion characteristics of a typical guide are shown in Figure 6.

2.2 Analysis of the Distributed Directional Coupler

A simple distributed directional coupler consists of a section of a coupled inverted stripguide of length ℓ and separation s, as shown in Figure 7. If port 1 is excited, the coupled energy is tapped off at port 3. Since no reflections are assumed, no energy is coupled into port 4. Using the above arguments, and with port 1 excited by an electric field of strength E_1,

$$E_{(1)}(0) = E_1 \qquad (26)$$

$$E_{(2)}(0) = 0 \qquad (27)$$

and for $0 < z < \ell$,

$$E_{(1)}(z) = E_e e^{-jk_e z} + E_o e^{-jk_o z} \qquad (28)$$

$$E_{(2)}(z) = E_e e^{-jk_e z} - E_o e^{-jk_o z} \qquad (29)$$

where $E_{(1)}(z)$, $E_{(2)}(z)$ are the fields along the guides I and II, at a distance z along the guide; E_e, E_o are fields of the even and odd modes of the coupled guide; and k_e, k_o are the propagation constants of the even and odd modes of the coupled guide.

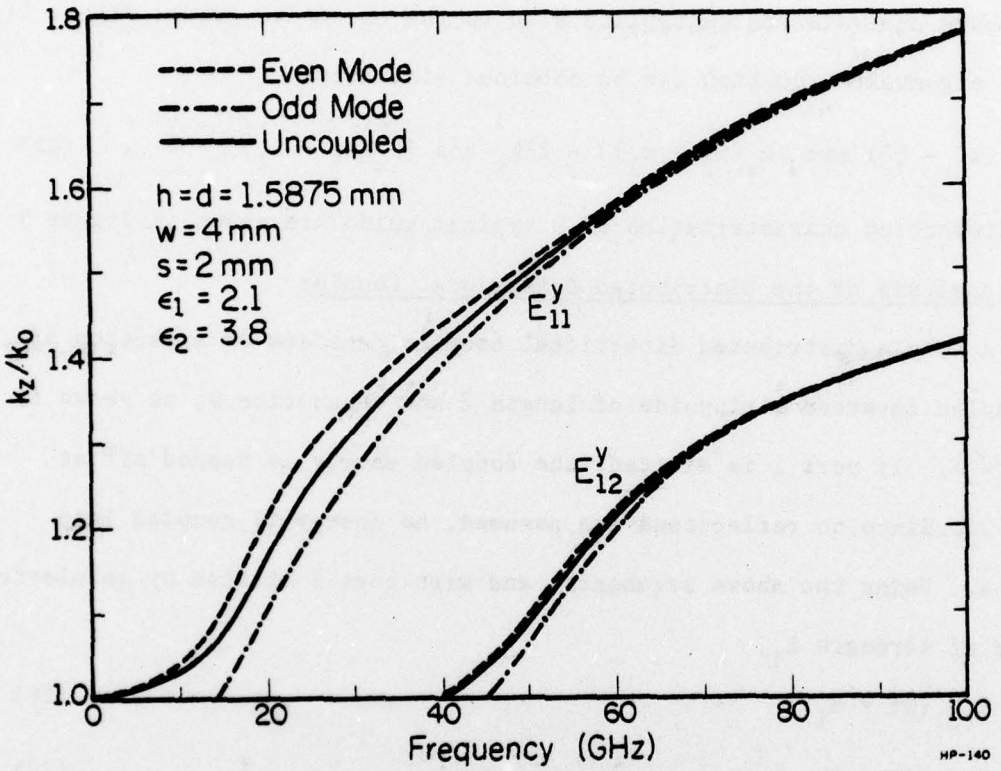

Figure 6. Relative propagation constant as a function of frequency for the uncoupled guide and the even and odd modes of the coupled guide.

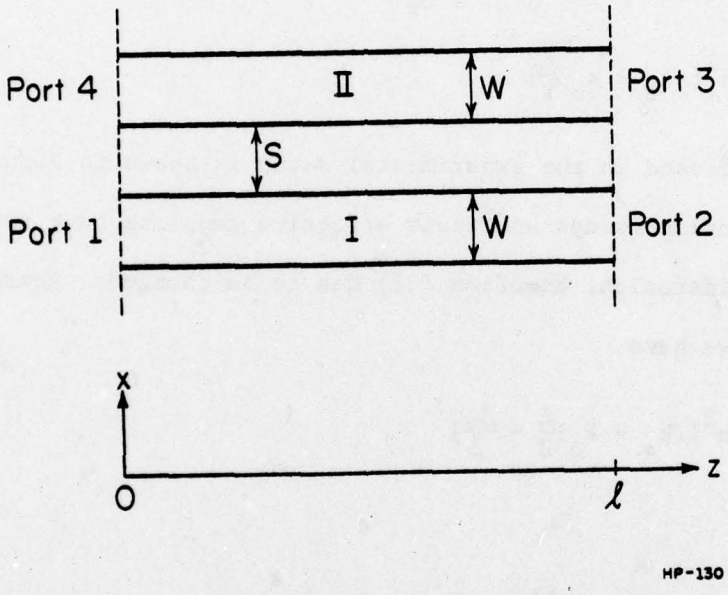

Figure 7. Isolated distributed directional coupler.

If the coupling length is ℓ, then the coupling is the ratio of the power in guides II and I, at $z = \ell$

$$\frac{P_3}{P_2} = \left[\frac{E_{(2)}(\ell)}{E_{(1)}(\ell)}\right]^2 \quad . \tag{30}$$

We know that if the coupler is symmetric about the z axis, the even and odd modes carry equal amounts of energy, hence, using Equations (28), (29) and (30), and letting $E_o = E_e$ with $z = \ell$, we have

$$\frac{P_3(\ell)}{P_2(\ell)} = \tan^2[(k_e - k_o)\frac{\ell}{2}] \quad . \tag{31}$$

The coupler used in the experimental setup is shown in Figure 8. Since the connecting guides and their effective coupling have not been taken into consideration, Equation (31) has to be changed. Rewriting Equation (31), we have

$$\frac{P_3(\ell)}{P_2(\ell)} = \tan^2[(k_e - k_o)\frac{\ell}{2} + \frac{\Delta\psi}{2}] \tag{32}$$

where

$$\frac{\Delta\psi}{2} = \int_{z_o}^{z^1} [k_e(z) - k_o(z)]\, dz \tag{33}$$

and z^1 is the value of z where $k_e \approx k_o$.

2.3 Analysis of the Ring Resonator

The inverted stripguide can be used to fabricate a simple single pole resonator. The resonator geometry is shown in Figure 9(a), along with its schematic diagram, Figure 9(b), which will aid in the analysis. As shown in Figure 9(b), each section of the guide on either side of the ring behaves like a distributed guide directional coupler. To simplify

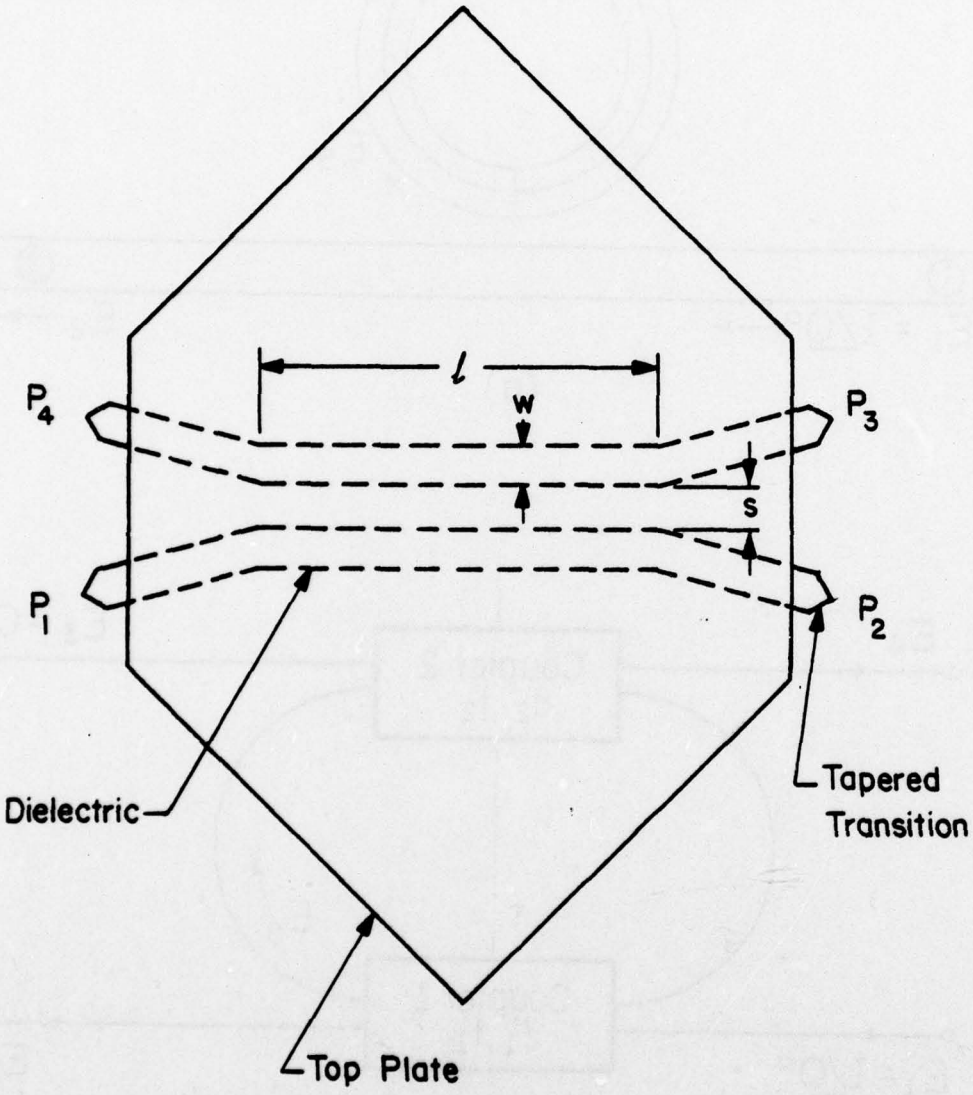

Figure 8. Top view of the directional coupler with the four connecting guides.

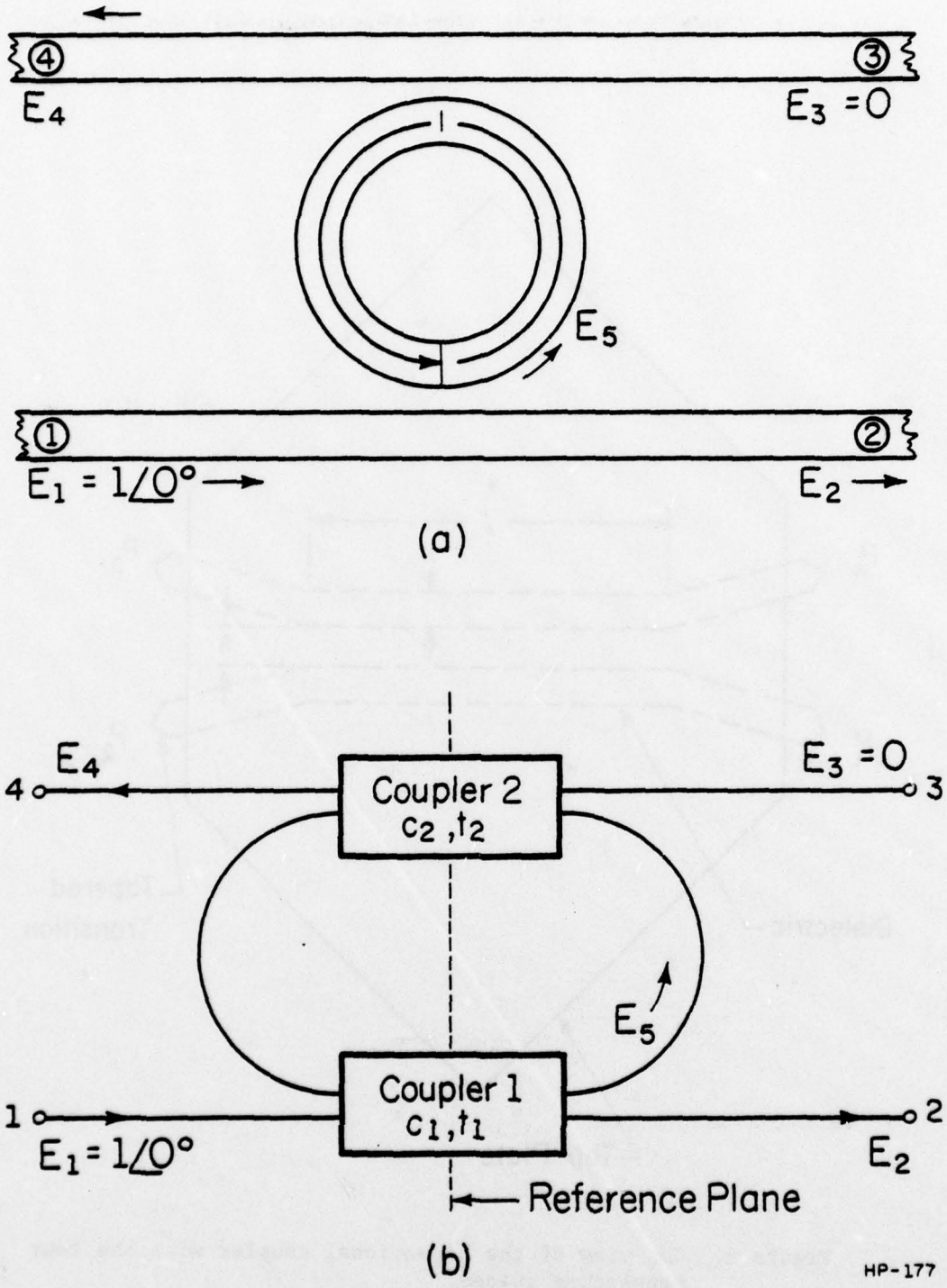

Figure 9. (a) Idealised ring resonator.
(b) Schematic diagram of ring resonator.

matters, we assume that all sections of the guide have identical characteristic impedances; that both directional couplers have infinite directivity, and are perfectly matched; that there are no points of reflection in the loop; and hence, a pure travelling wave exists.

Under these assumptions,

if

$$E_1 = 1e^{jo} \quad , \tag{34}$$

then

$$E_5 = c_1 + E_5 t_1 t_2 e^{-\gamma \ell} \tag{35}$$

or

$$E_5 = \frac{c_1}{1 - t_1 t_2 e^{-\gamma \ell}} \tag{36}$$

$$E_2 = \frac{t_1 - t_2 e^{-\gamma \ell}}{1 - t_1 t_2 e^{-\gamma \ell}} \tag{37}$$

$$E_3 = 0$$

$$E_4 = c_2 E_5 e^{-\gamma \ell/2} = \frac{c_1 c_2 e^{-\gamma \ell/2}}{1 - t_1 t_2 e^{-\gamma \ell}} \tag{38}$$

where, c_1, c_2 = complex coupling coefficients of couplers 1 and 2, respectively; t_1, t_2 = complex transmission coefficients of couplers 1 and 2, respectively; $\gamma = \alpha + \beta_g$, complex propagation constant in the ring; $\ell = 2\pi\bar{r}$ = mean ring circumference; $\bar{r} = \sqrt{ab}$ = mean ring radius, where a, b = inner and outer radii of the ring, respectively.

Now the condition for perfect rejection between ports 1 and 2 can be obtained by setting $|E_2| = 0$. The principal condition is obtained by assuming that the ring is lossless, i.e., $\alpha = 0$.

Then,

$$t_1 = t_2 e^{-j\beta_g \ell}. \tag{39}$$

For identical couplers, we must have $t_1 = t_2$, hence,

$$e^{-j\beta_g \ell} = 1 \tag{40}$$

which implies that

$$\ell = n\lambda_g \quad , \quad n = 0, 1, 2, \ldots \quad . \tag{41}$$

3. COMPONENT EVALUATION

3.1 Objective

The objective of the various experiments that were conducted was to determine whether the inverted stripguide can be used effectively in the construction of components for millimeter-wave integrated circuits. It can be shown that though the guide supports more than one mode, it can be made to behave as if it carries only the principal mode. Hence, to fabricate any component, one can apply the existing theory, which takes into account only the fundamental mode.

To ascertain that the dielectric guide is indeed effectively single-moded, two different inverted stripguides were considered, each of which theoretically supported more than one mode in the frequency range of interest (60-90 GHz). The first type of guide was the quartz-teflon guide, which had a central rib made of teflon, and the top plate of quartz. The second type of guide was the teflon-teflon guide, in which the central rib, as well as the top plate, were made of teflon. Components were fabricated, using the two types of guides on the assumption that only the fundamental mode was present. The experimental results were checked with the theory over a range of frequencies (79-84 GHz).

3.2 Rectangular Metal Waveguide to Dielectric Guide Transition

Figure 10 shows the tapered transition used for the metal-to-dielectric guide. A small section of the central rib, about 1 1/2 - 2 wavelengths, (ℓ in the figure) was tapered and inserted into the metal waveguide. Increasing the taper beyond this length increased the coupled energy only by a small amount. Typically, a taper of about 1 1/2 wavelengths

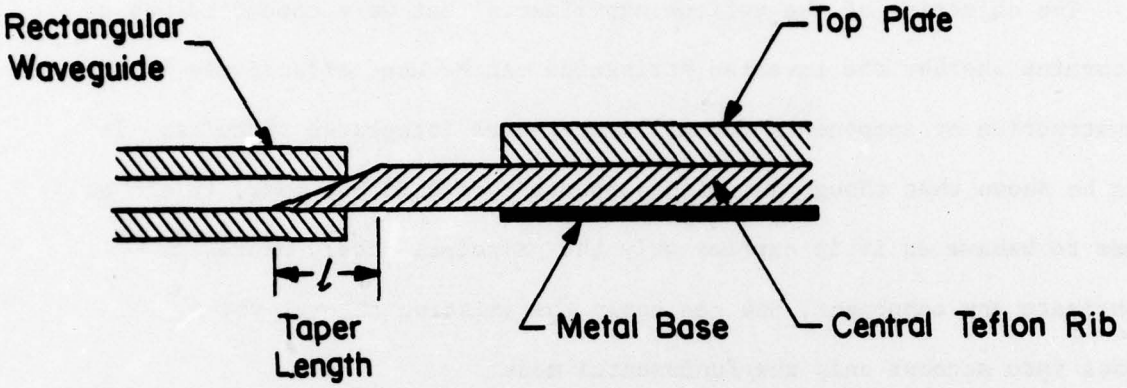

(a)

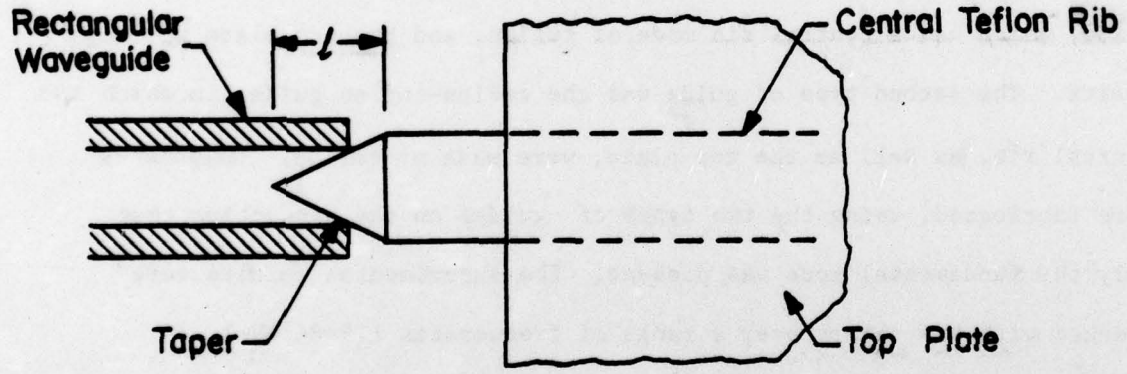

(b)

Figure 10. (a) Cross section of the side view of metal - dielectric guide transition.
(b) Top view of metal - dielectric guide transition.

(~4 1/2 mm at 80 GHz) gave fairly good results. This kind of taper is effective for both the quartz-teflon, and the teflon-teflon guide. Also, its simplicity of design makes it easy to fabricate. As the results show, the transition is very effective in that almost all the energy in the dielectric guide is confined to the fundamental mode.

3.3 Equipment Description

A schematic diagram of the setup is shown in Figure 11. A brief description of the various equipment is given below: The sweeper control unit, which comes with the sweeper source unit, was a Hughes' model 44017H sweeper control unit. The unit works in conjunction with a Hughes' sweeper source. The sawtooth input voltage was about 20-22 V, and the dc current was about 200 mA, varying by about 30 mA on both sides. The output bias current was such that the swept frequency was in the range of 79-84 GHz. The power output was about 5 mW.

The sweeper source unit, or the variable frequency oscillator was a tunable impatt oscillator, capable of being bias tuned over any interval in the range 77-87 GHz. The sawtooth current wave from the sweeper control unit establishes the swept frequency. The unit was a Hughes' model 41051H.

The modulator unit was a TRG E130; the detector was a Systron Donner DBH-319 with an IN53 diode mounted in it. A 1006 model, Micro-Tel logarithmic ratio meter was used for the measurements. This ensured that the y output of the X-Y plotter was linearly proportional to the decibel scale. A 202 A, Hewlett-Packard low-frequency function generator was used to monitor the input current into the sweeper control unit.

It must be noted that the combined nonlinearity of the system components over the 5 GHz bandwidth was <u>not</u> important, since the data

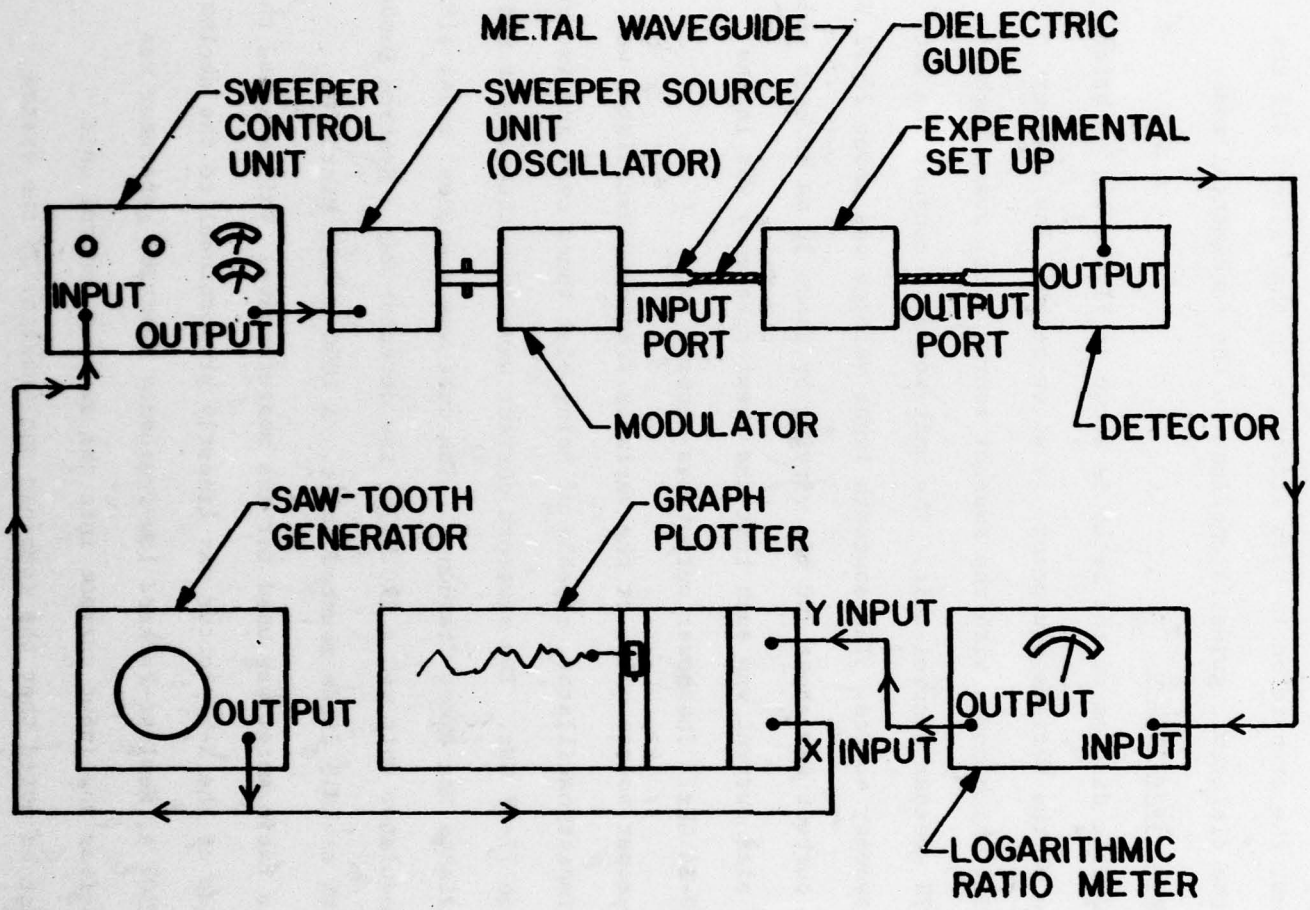

Figure 11. Schematic diagram of the experimental set-up.

are expressed as a ratio of the output signal through the device under test to the output signal with the device absent. There was another difficulty with the setup: the dc bias current output from the sweeper source would change perceptibly, when these two measurements (described above) were being made. Hence, the data had to be correctly interpreted, to obtain the results.

3.4 Distributed Directional Coupler Results

The distributed directional coupler on which the measurements were made is shown in Figure 8. Two sets of measurements were made: one on the quartz-teflon guide, and the other on the teflon-teflon guide. In the fabrication, care was taken to see that the angle between the coupled guide and the connecting guide was small (7° - 10°), in order to minimize losses by radiation. Also, at each transition, the sharp corners were smoothed out.

Two sets of measurements were made on each type of guide. The first set of measurements was the ratio of the relative power output of port 3 to port 2, i.e., (P_3/P_2), for various separations s, at a fixed frequency. The second measurement was concerned with the output ratio, P_3/P_2, as a function of frequency for different values of s. A typical measurement is shown in Figure 12. Here the lower curve is the relative power output from port 2, and the upper curve is the relative power output from port 3. Since the scale is in dB, the difference of the two curves gives the value of P_3/P_2 in dB. This is shown in Figure 13.

Figures 14 and 15 give a comparison of the theoretical and numerical results for various separations s for the two types of guides at a fixed frequency, 80 GHz. The experimental and theoretical results agree well for both cases. The agreement for small separations is not quite so good,

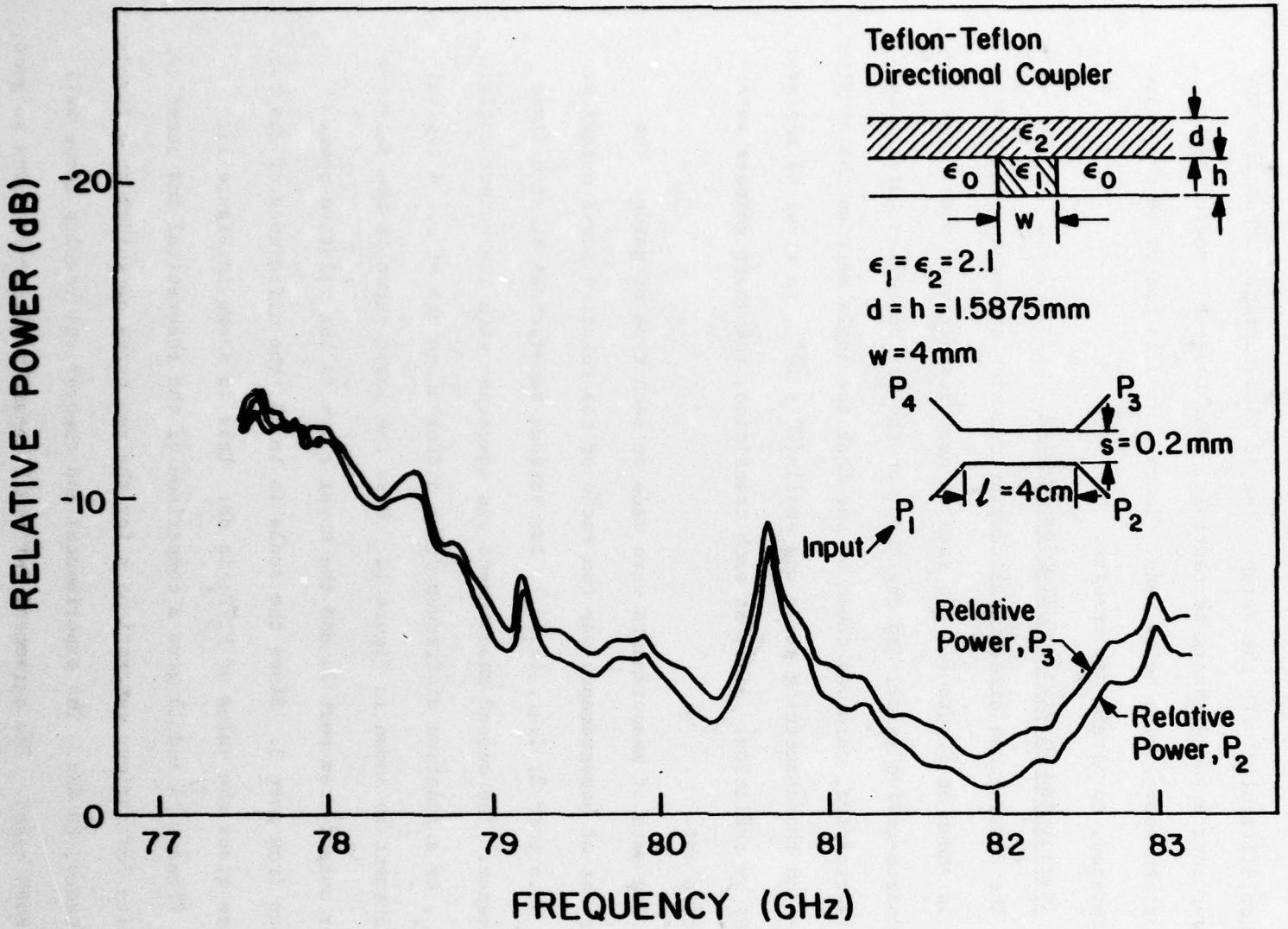

Figure 12. Typical measurement on a distributed directional coupler.

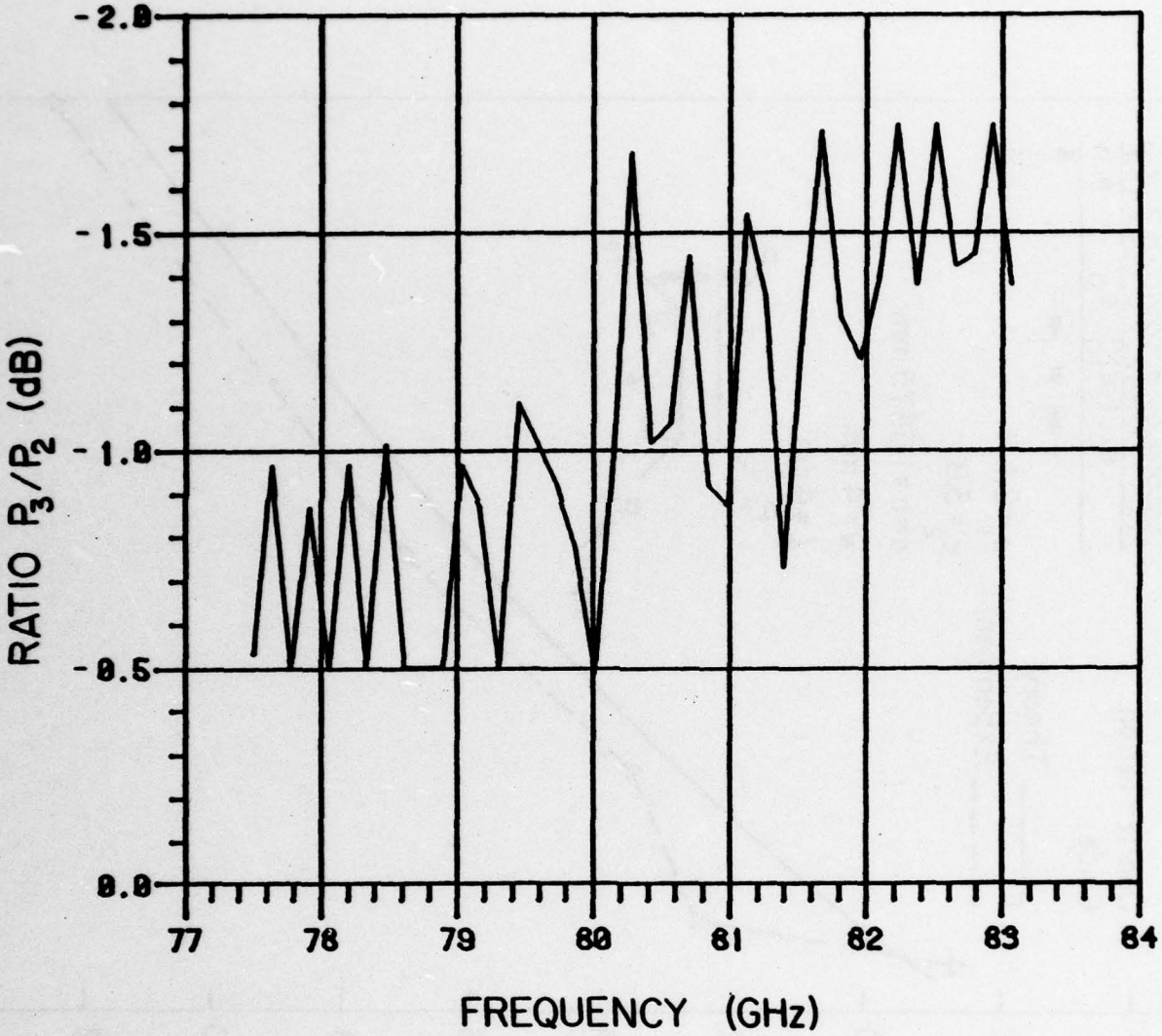

Figure 13. The ratio P_3/P_2 of the measurement taken in Figure 12.

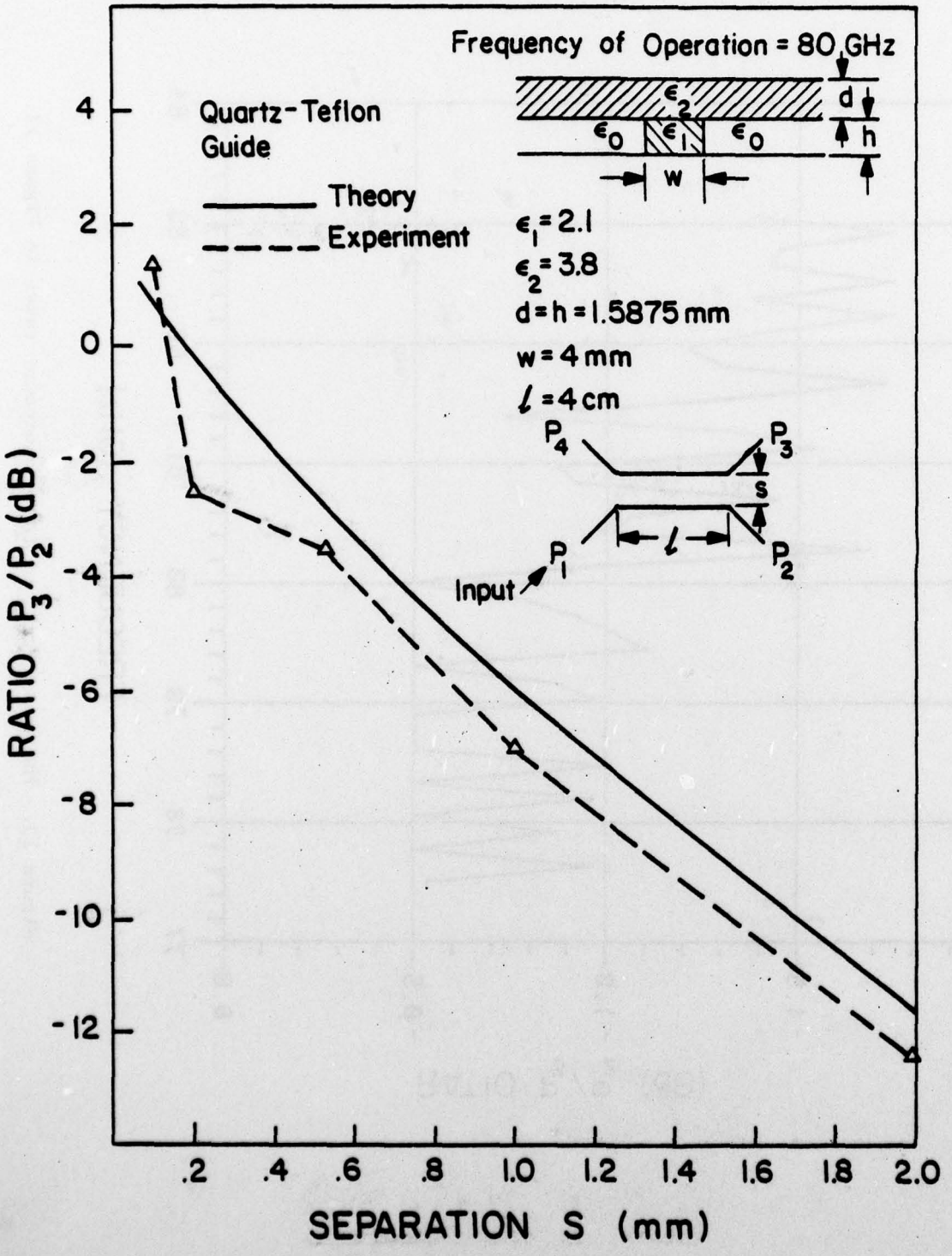

Figure 14. Comparison of theoretical and experimental results for the Quartz-Teflon distributed directional coupler.

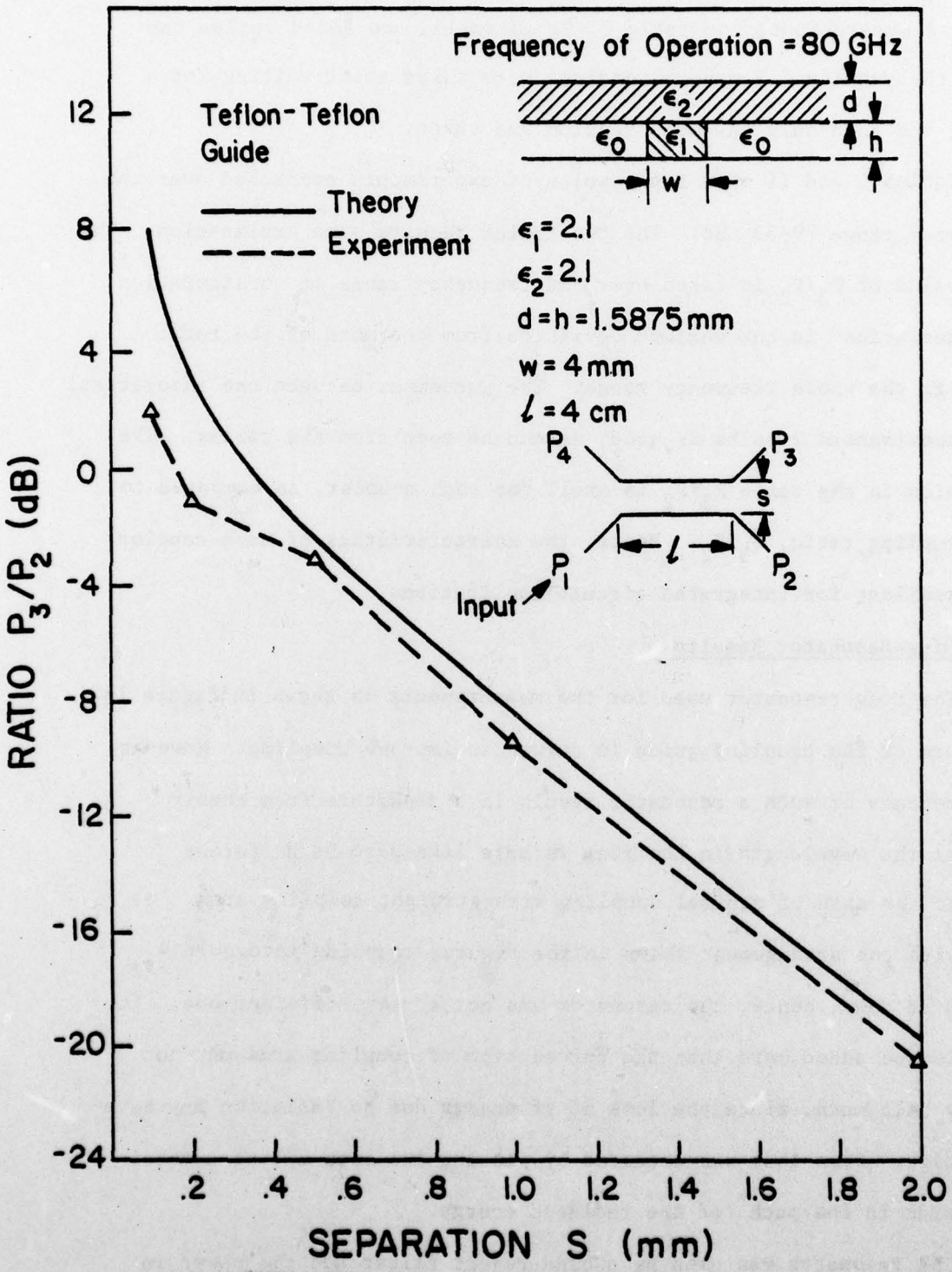

Figure 15. Comparison of theoretical and experimental results of the Teflon-Teflon distributed directional coupler.

since it becomes difficult to control the uniformity of the gap widths in the experiment, and hence, some error is bound to occur. In the case of large separations, the ratio P_3/P_2 is small, and noise spikes can upset the reading. However, readings were taken after waiting for a while, and then only the mean reading was taken.

Tables I and II show the results of experiments conducted over the frequency range 79-83 GHz. The two tables require some explanation. The mean value of P_3/P_2 is taken over the frequency range in consideration. The "deviation" is the maximum deviation from the mean of the ratio P_3/P_2 in the whole frequency range. The agreement between the theoretical and experimental results is good, as can be seen from the tables. The deviation in the ratio P_3/P_2 is small for each coupler, as compared to the coupling ratio, P_3/P_2. Hence, the characteristics of each coupler are excellent for integrated circuit applications.

3.5 Ring Resonator Results

The ring resonator used for the measurements is shown in Figure 16. Each arm of the coupling guide is curved to improve coupling. However, measurements on such a resonator result in a departure from theory in that the wavelength in the ring is more likely to be different than in the case of minimal coupling with straight coupling arms. Even with the arrangement shown in the figure, coupling into port 4 was 20 dB down, hence, the resonator was not a very efficient one. It may also be added here that the curved type of coupling arms may not really help much, since the loss of rf energy due to radiation may have been high. Some loss was detected by placing the open end of a metal waveguide in the path of the radiated energy.

The resonator was used as a band reject filter and the power in port 2 was compared to the input power. The resonance peaks were within

TABLE I. QUARTZ-TEFLON DIRECTIONAL COUPLER RESULTS

SEPARATION	THEORETICAL VALUE OF P_3/P_2 (dB)		EXPERIMENTAL VALUE OF P_3/P_2 (dB)	
S (mm)	MEAN P_3/P_2 FOR 79-83 GHz	DEVIATION IN P_3/P_2 FOR 79-83 GHz	MEAN P_3/P_2 FOR 79-83 GHz	DEVIATION IN P_3/P_2 FOR 79-83 GHz
0.2	-4.686	±0.388	-3.8	±0.5
1.0	-7.903	±0.312	-7.5	±0.5
2.0	-13.27	±0.173	-12.5	±1.0

TABLE II. TEFLON-TEFLON DIRECTIONAL COUPLER RESULTS

SEPARATION	THEORETICAL VALUE OF P_3/P_2 (dB)		EXPERIMENTAL VALUE OF P_3/P_2 (dB)	
S (mm)	MEAN P_3/P_2 FOR 79-83 GHz	DEVIATION IN P_3/P_2 FOR 79-83 GHZ	MEAN P_3/P_2 FOR 79-83 GHz	DEVIATION IN P_3/P_2 FOR 79-83 GHz
0.5	-2.995	±0.724	-1.125	±0.63
1.0	-8.836	±0.486	-8.5	±0.25
2.0	-19.458	±0.175	-20.0	±2.0

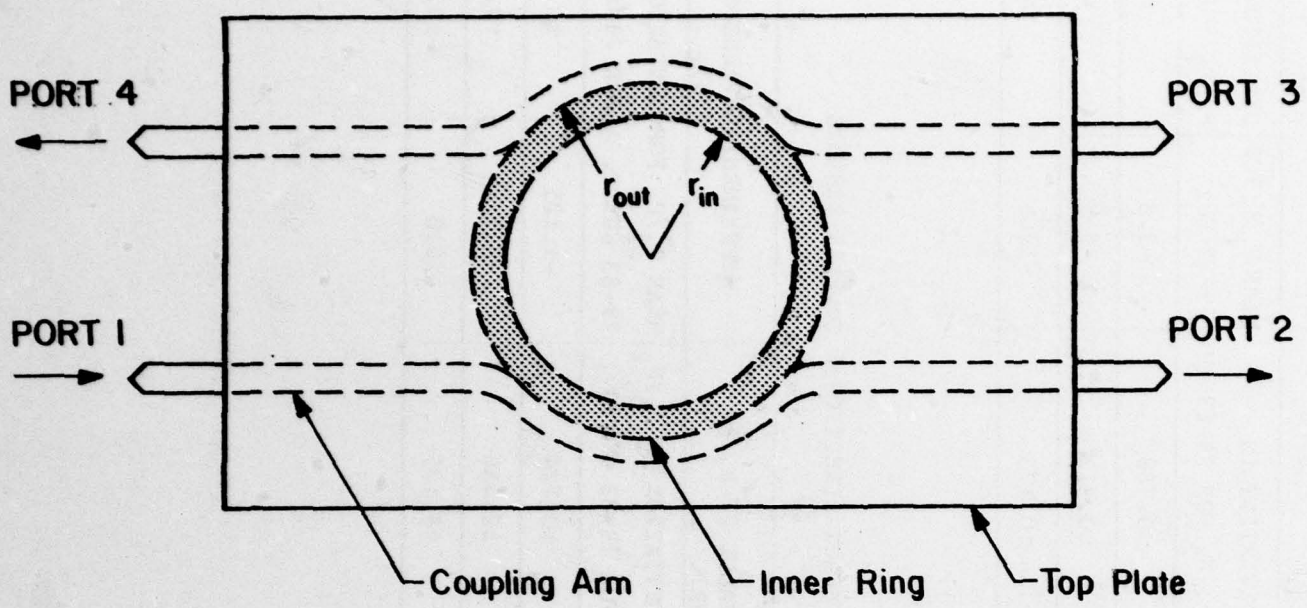

Figure 16. Top view of the ring resonator used for the experiment.

0.2 GHz of those predicted by the theory. The results have been tabulated in Table III.

3.6 Conclusion

Two passive devices were fabricated based on the assumption of a single mode. Agreement between theory and experiment was shown to be very good in the case of the quartz-teflon and the teflon-teflon inverted stripguides. Since the fundamental mode was considered in each guide, it is logical to conclude that practically all the energy was confined to the fundamental mode, the E_y^{11} mode. It is important to note that some other devices must be fabricated, and the above conclusion tested. Other devices that can be fabricated are the ferrite isolator and the beam splitter directional coupler.

There are a few main points to be noted. An improvement in VSWR must be attempted. Also, the ring resonator performance must be improved, if it is to be used as a band-pass or band-reject filter.

TABLE III. COMPARISON OF THEORETICAL AND EXPERIMENTAL RESULTS OF THE RING RESONATOR

$h = d = 1.5875$ mm $a = 15$ mm $\bar{r} = 16.882$ mm

$w = 4$ mm $b = 19$ mm $\varepsilon_1 = 2.1$

TYPE OF GUIDE	THEORETICAL RESONANCE FREQUENCY (GHz)	RESONANCE FREQUENCY OF EXPERIMENT (GHz)	DIFFERENCE (EXPT.-THEORY) (GHz)
QUARTZ-TEFLON $\varepsilon_2 = 3.8$	78.60	78.71	0.11
	80.00	80.19	0.19
	81.40	81.53	0.13
	82.80	82.95	0.15
TEFLON-TEFLON $\varepsilon_2 = 2.1$	77.80	78.10	0.30
	79.60	79.74	0.14
	81.60	81.75	0.15
	83.50	83.40	-0.10

REFERENCES

[1] D. Marcuse, Theory of Dielectric Optical Waveguides, New York: Academic Press Inc., 1974.

[2] W. V. McLevige, T. Itoh, R. Mittra, "New Waveguide Structures for Millimeter-Wave and Optical Integrated Circuits," IEEE Trans. Microwave Theory Tech., Vol. MTT-23, no. 10, pp. 788-794, October 1975.

[3] R. S. Rudokas, "Analysis of Inverted Strip Dielectric Waveguides and Passive Devices for Millimeter Waves," Coordinated Science Laboratory Report R-774, University of Illinois at Urbana-Champaign, July 1977.

[4] R. M. Knox and P. P. Toulios, "Integrated Circuits for the Millimeter Through Optical Frequency Range," Proceedings on the Symposium on Submillimeter Waves, New York, New York, March 31, April 1 & 2, 1970.

[5] T. Itoh, "Inverted Strip Dielectric Waveguide for Millimeter-Wave Integrated Circuits," IEEE Trans. Microwave Theory Tech., vol. MTT-24, no. 11, November 1976.

[6] R. F. Harrington, Time Harmonic Electromagnetic Fields, New York: McGraw-Hill, 1961.